N71-75336

4793-I

# III. PRELIMINARY ANALYSIS OF HYPERSONIC RAMJET COOLING PROBLEMS

By Henry R. Hunczak and George M. Low

## Introduction

One of the basic differences between flight at supersonic and hypersonic speeds lies in the temperatures encountered in these two flight regimes. At supersonic speeds, stagnation temperatures are sufficiently low so that internal components of ramjet engines upstream of the combustor do not have to be cooled. The hot parts of an engine (combustor and nozzle) can generally be film-cooled with ram air.

At hypersonic speeds, on the other hand, temperatures may reach a high enough level to make the cooling of all internal components mandatory. Furthermore, since the ram air will also be hot, it cannot be used as a coolant.

At sufficiently high speeds, therefore, all internal components of ramjet engines will have to be cooled either with an expendable coolant or regeneratively with the fuel; an alternative cooling scheme which transports the internally generated heat to the external surfaces, whence it can be radiated to the atmosphere, may also be feasible.

This paper presents the results of preliminary calculations of the heat loads sustained by ramjet engines in hypersonic flight. The heat-sink capacity of several fuels is examined, and the heat load is compared to the available cooling capacity.

## Symbols

| | |
|---|---|
| a | velocity of sound, ft/sec |
| h | enthalpy, Btu/lb |
| M | Mach number |
| Pr | Prandtl number |
| Q | heat load, Btu/sec |

36

Preceding page blank

[redacted]

| | |
|---|---|
| $q$ | heat-transfer rate, Btu/(sq ft)(sec) |
| $T$ | temperature, $^{\circ}R$ |
| $v$ | velocity, ft/sec |
| $x$ | distance parallel to surface from origin of boundary layer, ft |
| $\alpha$ | absorptivity of gas |
| $\varepsilon$ | emissivity of wall |
| $\varepsilon'$ | effective emissivity of wall, $(\varepsilon + 1)/2$ |
| $\varepsilon_g$ | emissivity of gas |
| $\nu$ | kinematic viscosity, sq ft/sec |
| $\rho$ | density, lb/cu ft |
| $\sigma$ | Stefan-Boltzmann constant, $0.48\times10^{-12}$ Btu/(sq ft)(sec)($^{\circ}R^4$) |

Subscripts:

| | |
|---|---|
| aw | adiabatic wall conditions |
| e | local conditions at outer edge of boundary layer |
| o | stagnation conditions at outer edge of boundary layer |
| w | wall or surface conditions |
| rad | radiation |
| ref | conditions evaluated at reference enthalpy as given in ref. 5 |
| 0 | free stream |

4793-I

## Calculation Procedure

The numerical calculations can, for convenience, be divided into two groups. The first comprises the inviscid-flow calculations which determine the internal aerodynamics and geometry of the configurations; the second group includes the viscous-flow and radiation analyses which are used to evaluate the heat loads.

[redacted]

Inviscid flow. - The free-stream conditions were based on the ICAO standard atmosphere as obtained from reference 1. For the supersonic inlet and subsonic diffuser the stagnation and local static pressures, temperature, and enthalpy for air were obtained by using real gas properties. Charts of these properties are published in reference 2.

For internal-compression inlets, isentropic one-dimensional flow was assumed with all flow losses occurring through a normal shock at the throat. For other inlet types, the oblique-shock losses were accounted for. At a Mach number of 7 and below, where the stagnation temperatures were below 5000° R, throat-shock Mach numbers were determined by using the methods of reference 3. These methods account for caloric imperfections but neglect gaseous imperfections such as dissociation. At a Mach number of 9, the stagnation temperatures were above 5000° R, and graphical solutions of the gas charts were used.

The diffuser-discharge Mach number was 0.2, at which point a stoichiometric fuel flow was added. The heat release was assumed to be instantaneous and was determined from the thermodynamic charts of reference 4. The momentum pressure loss due to combustion was neglected. However, for a free-stream Mach number of 7, calculations indicate that this loss is not large for a diffuser-discharge Mach number of 0.2.

The combustor length was held fixed at 2 feet, and the exhaust nozzles were assumed to be fully expanded.

Viscous flow. - Convective heat transfer: The convective heat loads were calculated using reference enthalpies (ref. 5) in the method outlined in reference 6 for turbulent boundary layers. A zero pressure gradient, variable property solution was employed in order to obtain preliminary results for comparison purposes. This simplified the analysis so that a wide range of variables could be investigated and trends could be established. The basic equation for the local heating rate is

$$q = 0.043\, \rho_e v_e (h_{aw} - h_w)\left(\frac{h_o}{h_e}\right)^{0.452}\left(\frac{h_e}{h_{ref}}\right)^{0.571}\left(\frac{M_e a_o}{\nu_o}\, x\right)^{-0.22}(Pr)_{ref}^{-2/3}$$

Sample calculations indicated that this equation yields results which are in excellent agreement with the semiempirical method of reference 5.

Flow properties, as previously indicated, were obtained from Mollier charts (refs. 2 and 4). Transport properties were obtained from the following sources:

(1) Prandtl number for air: Reference 7 for temperatures up to 4500° R; extrapolated values from 4500° to 6500° R.

[redacted]

(2) Viscosity of air: Reference 8 for temperatures up to 3400° R; above 3400° R viscosities were calculated by methods of reference 8 using self-diffusion coefficients.

(3) Prandtl number and viscosity for the combustion products of hydrogen and air: Calculated by methods proposed in reference 9.

For integration purposes the boundary layer was considered to originate at the cowl lip, the beginning of the subsonic diffuser, and the start of the combustor. The latter two assumptions were made because it was anticipated that some bleed would be required at the inlet throat, and the fuel nozzles and combustion process would disturb the boundary layer sufficiently to wipe a large part of it away.

The majority of the calculations were made for wall temperatures of 2000° R in the inlet and subsonic diffuser and 2500° R in the combustor and exhaust nozzle. Heat-transfer calculations for different temperatures were made by changing only the wall enthalpy in the heat-transfer equation; the effects of this change on reference enthalpy and Prandtl number were neglected. (This assumption is equivalent to assuming that the heat-transfer coefficient is independent of surface temperature.)

Radiation heat transfer: Radiation from the hot stream to the cold wall contributes to the heat transfer when water vapor or carbon dioxide is present. Since hydrogen fuel was used in the heat-transfer analysis, only water vapor contributed to the radiation heat load in the combustor and exhaust nozzle.

Calculation procedures suggested in references 10 to 12 were employed. The equation for radiation heat flux is

$$q_{rad} = \sigma \epsilon_w' (\epsilon_g T_e^4 - \alpha T_w^4)$$

An emissivity of 0.35 was assumed for the wall.

Although the local convective heat loads could be scaled with engine size, the radiation heat load cannot be scaled. Instead, radiation heat-transfer rates were recalculated for each of the altered conditions investigated.

Total heat load: Total heat loads were obtained by a planimeter integration of a plot of the local heat-transfer rate as a function of the wetted surface area.

[redacted]

## Results and Discussion

Representative engine. - In order to study the effect of the variation of many parameters on the heat load, a representative engine was selected (fig. 1). An internal-compression inlet was chosen in order to facilitate the computations. The combustor length was fixed at 2 feet, while the combustion-chamber Mach number equaled 0.2. An inlet diameter of 10 feet was assumed for many of the calculations. All other pertinent dimensions are given in figure 1.

Temperatures and heat flux. - External temperatures: If the engine is free to radiate in all directions, the external surfaces will assume an equilibrium temperature which results when the aerodynamic heat input is balanced by the heat radiated away from the engine.

Typical radiation equilibrium temperatures for an emissivity of 0.8 are presented as the dashed curves of figure 2. With the exception of a small region near the leading edge, these temperatures are sufficiently low to make the cooling of external surfaces unnecessary. At a constant Mach number, radiation equilibrium temperatures decrease with increasing altitude. From external temperature considerations, therefore, it is beneficial to fly at the highest possible altitude.

Internal temperatures: The internal temperature distributions of an uncooled engine are also shown in figure 2. As the Mach number increases, these temperatures become intolerably high in all parts of the engine. Because these high temperatures exceed the limits of all known materials, all internal components require some form of cooling. The question then arises as to the rate at which heat must be carried away in order to maintain allowable temperatures.

Internal heat-transfer rates of cooled engine: The heat-transfer rate, or heat flux, of the representative engine is presented in figure 3. The curve is for flight at Mach 9 and an altitude of 140,000 feet; hydrogen fuel was used for this calculation. Wall temperatures in the inlet and subsonic diffuser were assumed to be 2000° R; in the combustor and exhaust nozzle, where oxidation problems do not exist, a wall temperature of 2500° R was assumed.

High heat fluxes occur in the throat regions and in the combustion chamber (fig. 3). But even at this very high Mach number, the peak heat-transfer rate is only about 400 Btu/(sq ft)(sec). This heat flux is about 25 percent of the heat-transfer rates currently being handled successfully in rocket motors. It should, therefore, be possible to cool ramjet engines in hypersonic flight without serious difficulties.

Regenerative cooling system. - The magnitude of the heat flux suggests that a regenerative cooling system be used which makes use of the fuel as

[redacted]

a coolant. The cooling capacities and impulses of several fuels are shown in the following table:

| Fuel | Minimum temperature, $^{\circ}$R | Maximum temperature, $^{\circ}$R | Relative specific impulse | Relative cooling capacity | |
|---|---|---|---|---|---|
| | | | | Inlet and subsonic diffuser | Combustor and nozzle |
| Hydrogen | 37 | 2500 | 100 | 100 | 100 |
| Diborane | 194 | 600 | 45 | 5.4 | 10.2 |
| Ethyl decaborane | 520 | 760 | 38 | 2.0 | 2.7 |
| Methane | 201 | 1520 | 35 | 15.2 | 28.6 |
| Stable JP type | 520 | 1060 | 31 | 5.4 | 11.5 |

Results in this table are for stoichiometric fuel-air ratio and flight at Mach 7 with the engines scaled to provide equal internal thrust. The minimum temperatures for the cryogenic fuels are their boiling point. The maximum temperatures for all fuels except hydrogen were determined from limits imposed by the degradation of the fuel; hydrogen has no such limit, and the material temperature limit of 2500$^{\circ}$ R was, therefore, chosen as a maximum.

The relative cooling capacity is a function not only of the heat-sink capacity of the fuel but also of the relative heat load of the several fuels. The heat-sink capacity is related to both the specific heat of the fuel and the temperature rise during the cooling process. The heat load depends on the heat-transfer coefficient, the surface area, and the enthalpy of the gas (air or combustion products) at the wall and adiabatic wall temperatures. The difference in relative cooling capacities of the cold parts (inlet and diffuser) and the hot parts (combustor and nozzle) of the engine is due to the different enthalpies of air and of the products of combustion. Heat-transfer coefficients were not adjusted for the different fuel types.

When compared with hydrogen, the cooling capacities of the two boron fuels and the jet fuel are very low. This fact stems from a combination of a low specific heat and a low allowable temperature rise. Methane, which has an impulse somewhat better than that of jet fuel, has also a somewhat better cooling capacity. The two cooling capacities of methane (28.6 for the combustor plus nozzle and 15.2 for the inlet and diffuser) can be combined into a single value if the proportion of the total heat load in each engine component is known. If it is assumed that three-quarters of the total heat load is in the combustor and nozzle, and one-quarter is in the inlet and diffuser, the over-all cooling capacity of methane is 25 percent that of hydrogen. This may be sufficient for some

4793-I

[redacted]

applications. But when both cooling capacity and impulse are considered, none of the fuels measures up to hydrogen. All the subsequent heat-transfer calculations were, therefore, based on hydrogen fuel.

Of course, not all the heat-sink capacity of the fuel is available to cool the engine. In a regenerative cooling scheme the engine walls become a rather complex heat exchanger. An analysis has shown that such a heat exchanger using hydrogen fuel can be 80 to 85 percent efficient at Mach 7. In addition, some of the cooling capacity may be required to cool the airplane structure, the instruments, and the payload. These other uses, together with the 15- to 20-percent heat-exchanger losses, have led to the assumption that 50 percent of the fuel cooling capacity is available to cool the engine.

Total heat load. - The heat flux throughout the engine was integrated to yield the total heat load. The effects of Mach number, altitude, and pressure recovery were investigated for the engine with an internal compression inlet. An inlet diameter of 10 feet and wall temperatures of 2000° R in the inlet and diffuser and 2500° R in the combustor and nozzle were chosen. Next, the effect of wall temperature was investigated for the same 10-foot engine; the effect of engine size was also calculated. Finally, the effect of other inlet types on total heat load was analyzed.

Effect of Mach number: In figure 4 the heat load, relative to the cooling capacity, is plotted as a function of Mach number. An altitude schedule corresponding to a constant dynamic pressure of 400 pounds per square foot and a pressure recovery schedule corresponding to a kinetic energy efficiency of about 92 percent were chosen. If 50 percent of the heat-sink capacity of the hydrogen fuel is available to cool the engine, a limiting Mach number of slightly over 8 can be reached.

Effect of altitude: It is well known that the heat load decreases with increasing altitude. But, for a fixed inlet size, the airflow (and hence, the fuel flow) decreases with increasing altitude; this causes a reduction in heat-sink capacity. The net result is that the heat load increases relative to the cooling capacity as the altitude is increased. However, as shown in figure 5, this increase is not very pronounced at Mach 7.

Effect of total-pressure recovery: The effect of total-pressure recovery for a family of similar internal compression inlets is rather interesting in that two opposing factors are of importance. As the pressure recovery is increased, the local heat flux increases. But at the same time the wetted areas of the subsonic diffuser, the combustor, and the exhaust nozzle are reduced. The resulting total heat load is shown in figure 6. For the conditions of these calculations, the heat load peaks at a pressure recovery between 0.15 and 0.18. But the over-all effect of pressure recovery (for geometrically similar engines) is very small.

[redacted]

Effect of metal surface temperature: Up to this point all results were presented for the rather high surface temperatures of 2000° R in the inlet and subsonic diffuser and 2500° R in the combustor and exhaust nozzle. Although these temperatures are high, they are not completely unrealistic; alloys are now being developed that have satisfactory strength at temperatures approaching 2500° R.

However, if the high temperatures cannot be maintained, it is still possible to cool the engine by using a larger portion of the cooling capacity of the fuel. The effect of surface temperature on the ratio of heat load relative to cooling capacity is shown in figure 7. This ratio increases with decreasing surface temperature for two reasons: First, the local heat flux is increased as the difference between the wall and the adiabatic wall temperatures increases; second, the heat-sink capacity of the fuel decreases as the maximum fuel temperature decreases.

If only 50 percent of the heat-sink capacity of the fuel is available to cool the engine, the minimum allowable surface temperature is about 2000° R (fig. 7). This minimum can be decreased slightly by applying a high-temperature insulating coating, as shown by the dashed line in figure 7. A 0.05-inch coating of zirconia can be used to reduce the average metal surface temperature by about 100° without raising the heat load. (The previously mentioned numbers, of course, apply only at the specified conditions: namely, $M_0$, 7; altitude, 120,000 ft; inlet diameter, 10 ft; fuel, hydrogen.)

The penalty for applying a high-temperature coating is the resulting increased engine weight. The 0.05-inch coating, when applied to the reference engine, adds 30 to 40 percent to its weight. In a practical application, therefore, coatings should be applied only in regions of high heat flux, because they are most effective in these regions.

Effect of engine size: So far all results were for an engine with the rather large inlet diameter of 10 feet. An engine of this size may be required for missions of semiglobal range. But for shorter ranges, such as the intercontinental mission, smaller engines are wanted. The effect of engine size at a Mach number of 7 and an altitude of 120,000 feet and with hydrogen fuel is shown in figure 8. The heat load increases rather rapidly relative to the cooling capacity as the engine size is decreased. For 50-percent heat-sink utilization the minimum allowable inlet diameter is 4 feet.

Comparison of several inlet types: As mentioned earlier, the parametric study of heat loads was made for an engine with an all-internal-compression inlet. In order to start and control this inlet, rather large area variations are required. The problem of cooling large movable components is exceedingly difficult. Also, with this type of inlet, large quantities of hot boundary-layer bleed flow must be handled. The inlet therefore does not appear to be very practical for application at high hypersonic speeds.

[redacted]

In figure 9(a) the total heat loads of several other inlet types are shown. These inlets are drawn schematically in figure 9(b). All engines were sized for equal thrust at a Mach number of 7 and an altitude of 120,000 feet. The inlet types are described in the following table:

| Engine | Inlet type | Total-pressure recovery |
|---|---|---|
| A | Internal compression | 0.12 |
| B | Three-dimensional isentropic spike, external compression | 0.12 |
| C | Three-dimensional isentropic spike, rapidly expanding diffuser | 0.12 |
| D | Three-dimensional isentropic spike, external plus internal compression | 0.25 |
| E | Two-dimensional isentropic wedge, external compression | 0.12 |
| F | Two-dimensional isentropic wedge, external plus internal compression | 0.12 |
| G | Two-dimensional single wedge | 0.04 |

4793-I

Engine A is the reference engine with the internal compression inlet. Its total heat load is unity. About one-half of the heat load is in the exhaust nozzle, one-fourth in the combustion chamber, and the remainder in the inlet and subsonic diffuser. The total load is relatively low because the regions of high heat flux occur where the surface areas are small. (Surface areas in square feet are indicated by the numbers in fig. 9(b)).

Engine B is three dimensional with an isentropic external-compression inlet. The supersonic inlet has a very low heat load because it can radiate to the atmosphere. The subsonic diffuser, on the other hand, has a very high heat load that results from a large surface area in a region of high heat flux.

The heat flux in the subsonic diffuser can be minimized by providing a rapid area expansion or perhaps by allowing the flow to separate. Engine C is identical to engine B, with the exception that the area in the subsonic diffuser is expanded rapidly. The heat load for this component was computed with the assumption that the flow remains attached. With this modification, the total heat load of the inlet with external compression is slightly less than that of the internal-compression inlet.

Engine D represents another modification of engine B. The pressure recovery was increased from 0.12 to 0.25 by incorporating some internal compression in addition to the external compression. This modification

[redacted]

increased the heat load in the supersonic inlet and decreased the nozzle heat load. The changes in the subsonic diffuser and combustor heat loads were minor. The total heat load of engine D is somewhat higher than that of engine B.

Engines E and F both have two-dimensional inlets with isentropic compression surfaces. Engine E has all external compression, while engine F has combined internal and external compression. Pressure recoveries of 0.12 were assigned to both inlets. The internal compression again raises the heat load of the supersonic inlet. The total heat load of engine E is about 30 percent higher than that of engine A, while the heat load of engine F exceeds that of the reference engine by 50 percent.

4793-I

Engine G has a two-dimensional single-wedge inlet with a total-pressure recovery of 0.04. Its total heat load is relatively low and can probably be reduced further by modifying the subsonic diffuser.

Closed cooling cycle. - It has been shown that at Mach 5 only about 15 percent of the cooling capacity of hydrogen is needed to cool the engine. Therefore, methane might also be satisfactory for cooling up to Mach 5 or perhaps even Mach 6. But at Mach 7 and above, more than 30 percent of the cooling capacity of hydrogen is required for the engine alone. None of the other fuels that were considered have even this much cooling capacity with stoichiometric combustion. From cooling considerations it must therefore be concluded that hydrogen is the only practical fuel for flight at high hypersonic speeds if a regenerative cooling system is to be used.

A different type of cooling system not using the fuel as a coolant was also investigated. It was shown in figure 2 that the external surfaces of the engine are at temperatures below the material limits. It may therefore be possible to transport the internal heat to the external surfaces and to radiate it to the atmosphere. This system is shown schematically in the upper part of figure 10. The heat picked up along the internal surfaces is carried to the external surfaces through a heat exchanger, probably of the liquid-metal type. A pump for the heat-exchanger agent is also required.

The performance of this system is shown in the lower part of figure 10. The dashed line represents the heat to be removed for the conditions indicated at the top of the figure. If the external surfaces can be maintained at a temperature of 2400° R, the system is good at Mach numbers even above 9. But the 2400° R temperature allows for only a 100° temperature drop in the heat exchanger; this may be very unrealistic. If the external temperature is kept at 1900° R, the closed cooling cycle cannot be used at Mach numbers much above 5. These results should, however, be qualified. First of all, they apply only for a very specific set of conditions. Second, the external engine surface area was used as a radiator

[redacted]

surface. This area would be decreased if the engine is not free to radiate in all directions; it could also be increased by using other parts of the aircraft surfaces as radiators.

The system has some inherent disadvantages. It would probably be quite heavy. All parts of the engine structure would be very much hotter than in a fuel-cooled system. The development of a liquid-metal pump is also required.

If hydrogen fuel is acceptable, a regenerative cooling scheme is probably the simplest and most practical. If for some reason the use of hydrogen is ruled out, a cooling cycle such as shown in figure 10 will have to be developed.

## CONCLUDING REMARKS

The results of a preliminary study of the cooling requirements of ramjet engines have been presented. Although the general trends and approximate magnitudes of these results are believed to be correct, the exact values and cooling limits are probably a function of the assumptions inherent in the analysis.

Perhaps one of the major assumptions lies in the use of a stoichiometric fuel-air ratio. The cooling capacity is almost directly proportional to fuel-air ratio. Therefore, all the cooling limits can be increased by burning at equivalence ratios greater than 1; of course, the specific impulse is thereby decreased.

The low bleed flow requirements and the absence of moving parts suggest the use of an external-compression inlet for flight at high hypersonic speeds. The cooling requirements of this inlet need not exceed those of an internal-compression inlet.

At Mach numbers of 7 and above, regenerative cooling is probably the simplest and most practical scheme. Fuels such as jet fuel, diborane, and ethyl decaborane are ruled out because of their almost negligible cooling capacity. Methane may give satisfactory performance up to some low hypersonic speeds.

The calculated results indicate that hydrogen fuel is outstanding for the purpose of regenerative cooling at Mach 7 and above, in that it has both a high heat capacity and a high heat of combustion.

[redacted]

## REFERENCES

1. Air Force Cambridge Research Center: Atmospheric Models. Doc. No. 56SD233, Missile and Ord. Systems Dept., General Electric, Phila. (Pa.).

2. Moeckel, W. E., and Weston, Kenneth C.: Composition and Thermodynamic Properties of Air in Chemical Equilibrium. (To be published.)

3. Ames Research Staff: Equations, Tables, and Charts for Compressible Flow. NACA Rep. 1135, 1953. (Supersedes NACA TN 1428.)

4. Hall, Eldon W., and Weber, Richard J.: Tables and Charts for Thermodynamic Calculations Involving Air and Fuels Containing Boron, Carbon, Hydrogen, and Oxygen. NACA RM E56B27, 1956.

5. Eckert, E. R. G.: Engineering Relations for Friction and Heat Transfer to Surfaces in High Velocity Flow. Jour. Aero. Sci., vol. 22, no. 8, Aug. 1955, pp. 585-587.

6. Reshotko, Eli, and Tucker, Maurice: Approximate Calculation of the Compressible Turbulent Boundary Layer with Heat Transfer and Arbitrary Pressure Gradient. NACA TN 4154, 1957.

7. Glassman, Irvin, and Bonilla, Charles F.: The Thermal Conductivity and Prandtl Number of Air at High Temperatures. Preprints of papers for Heat Transfer Symposium, Am. Inst. Chem. Eng., Dec. 1951.

8. Hilsenrath, Joseph, et al.: Tables of Thermal Properties of Gases. Cir. 564, NBS, Nov. 1, 1955.

9. Hirschfelder, Joseph O., Curtiss, Charles F., and Bird, R. Byron: Molecular Theory of Gases and Liquids. John Wiley & Sons, Inc., 1954.

10. McAdams, William H.: Heat Transmission. Second ed., McGraw-Hill Book Co., Inc., 1942.

11. Hottel, A. C.: Radiant Heat from Water Vapor. Trans. Am. Inst. Chem. Eng., vol. 38, 1942, p. 531.

12. Penner, S. S., and Thomson, A.: Determination of Equilbrium Infrared Gas Emissivities from Spectroscopic Data. Presented at Second Biennial Gas Dynamics Symposium, Tech. Inst., Northwestern Univ., Aug. 26-28, 1957.

4793-I

[redacted]

## REPRESENTATIVE ENGINE USED IN HEAT-TRANSFER ANALYSIS

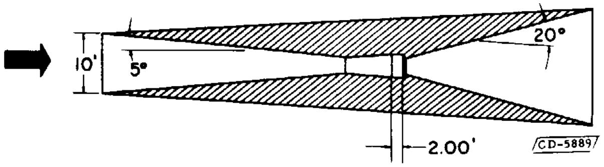

Figure 1

## EQUILIBRIUM TEMPERATURES OF UNCOOLED ENGINE

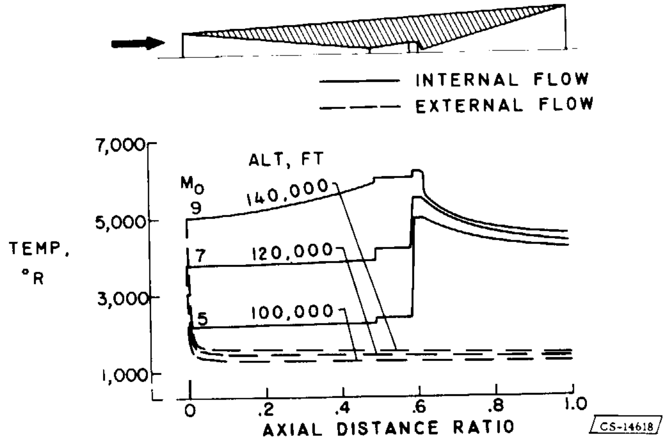

Figure 2

## LOCAL INTERNAL HEAT TRANSFER RATES OF COOLED ENGINE

$M_0$, 9, ALTITUDE, 140,000 FT

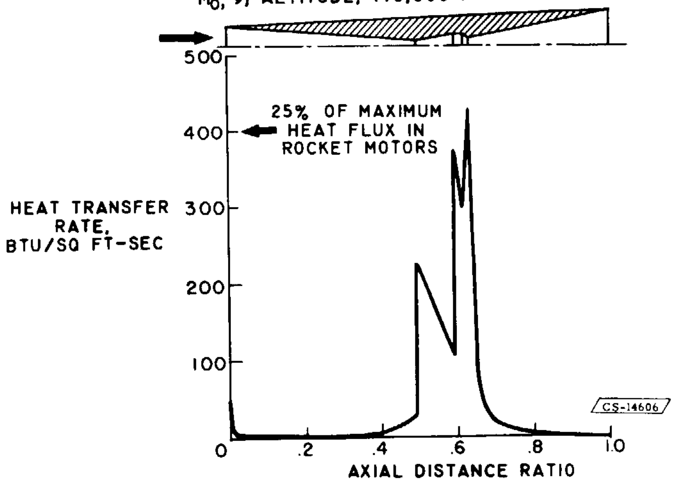

Figure 3

## INCREASING MACH NUMBER RAISES HEAT LOAD

FUEL, HYDROGEN, $D_{INLET}$, 10 FT, DYNAMIC PRESSURE, 400 PSF

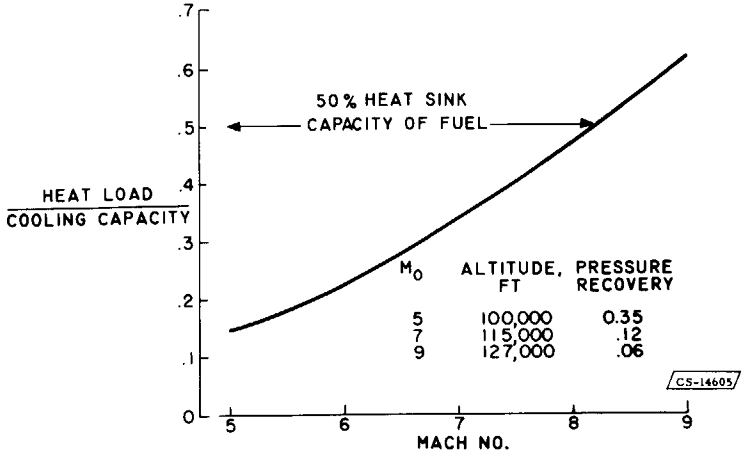

Figure 4

## HIGHER ALTITUDE REDUCES COOLING RESERVE

$M_0$, 7, $D_{INLET}$, 10 FT, FUEL, HYDROGEN

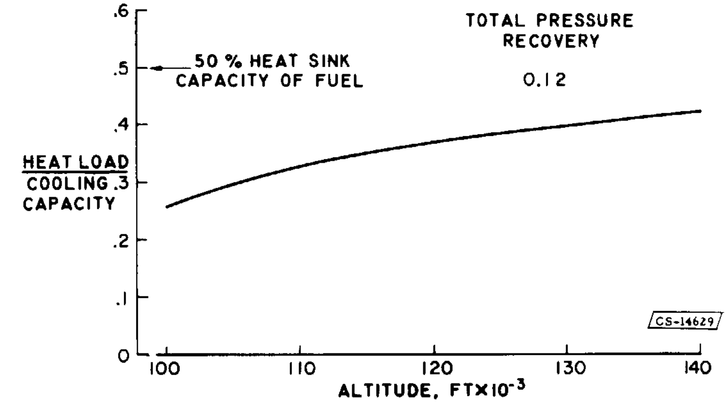

Figure 5

## EFFECT OF TOTAL-PRESSURE RECOVERY ON HEAT LOAD

($M_0$, 7, $D_{INLET}$, 10 FT, FUEL, HYDROGEN, ALT, 120,000 FT)

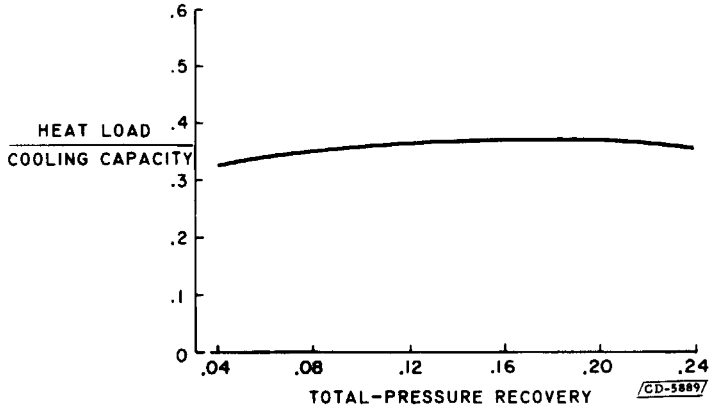

Figure 6

## LOWER SURFACE TEMPERATURE YIELDS HIGHER HEAT LOAD

$D_{INLET}$, 10 FT, $M_0$, 7, ALTITUDE, 120,000 FT, FUEL, HYDROGEN

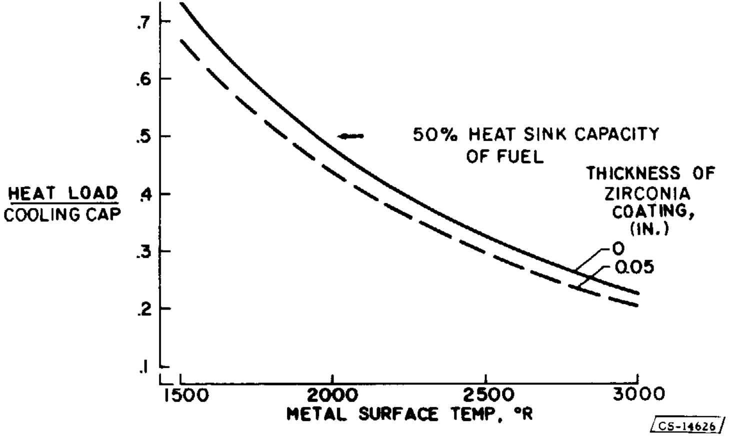

Figure 7

## LARGE ENGINES ARE EASIER TO COOL THAN SMALL ONES

$M_0$, 7; ALTITUDE, 120,000 FT, HYDROGEN FUEL

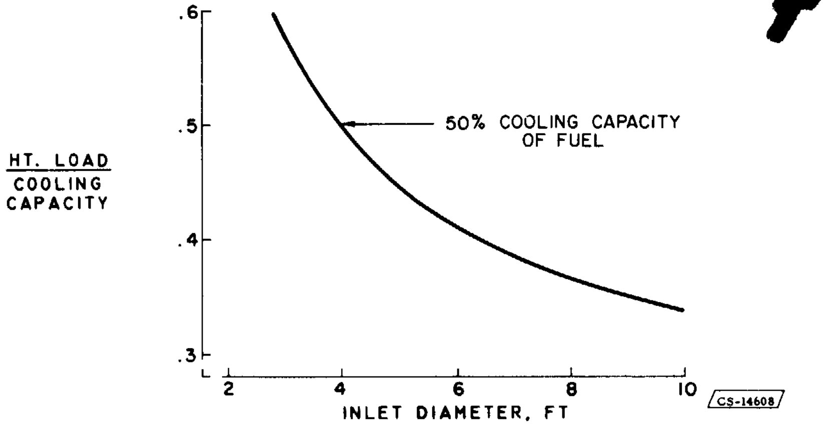

Figure 8

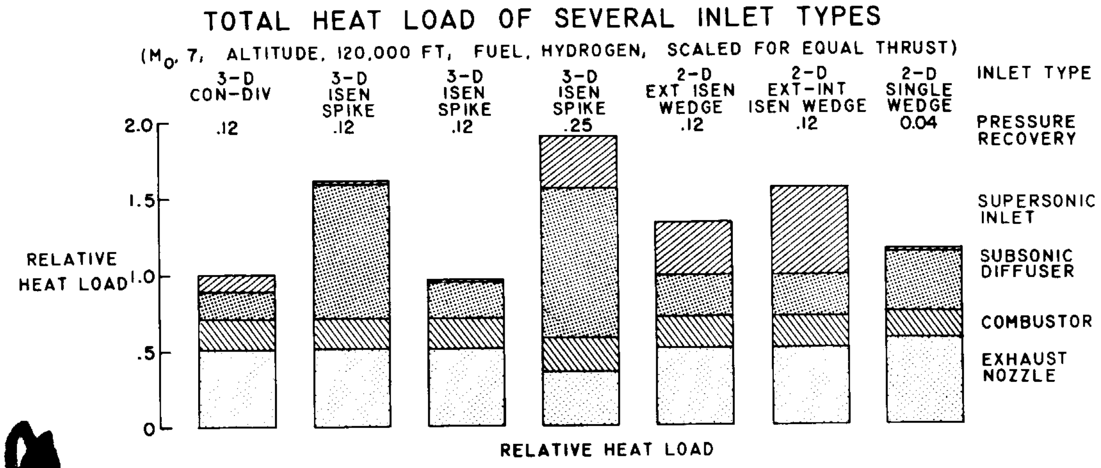

Figure 9(a)

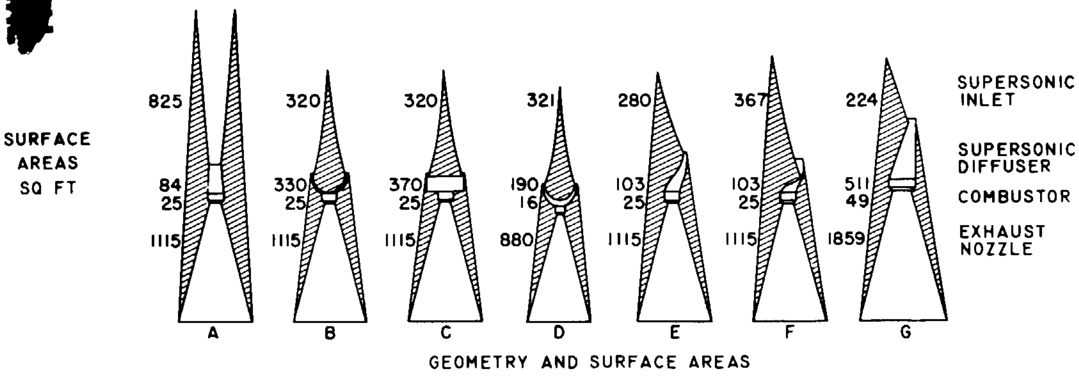
SURFACE AREAS SQ FT
825
84
25
1115
A
320
330
25
1115
B
320
370
25
1115
C
321
190
16
880
D
280
103
25
1115
E
367
103
25
1115
F
224
511
49
1859
G
SUPERSONIC INLET
SUPERSONIC DIFFUSER
COMBUSTOR
EXHAUST NOZZLE
GEOMETRY AND SURFACE AREAS

Figure 9(b)

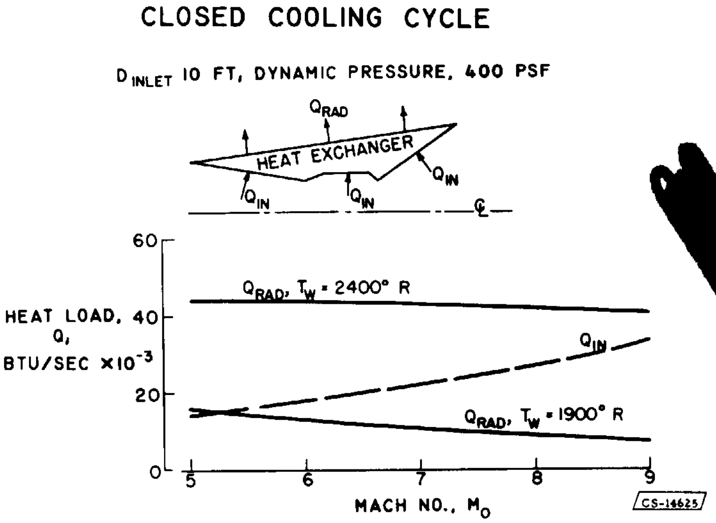

Figure 10